Available online at www.sciencedirect.com
SCIENCE DIRECT®
Optical Fiber Technology 11 (2005) 332–345
Optical Fiber Technology
www.elsevier.com/locate/yofte

W-type fiber design for application in U- and S-band amplifiers by controlling the LP_{01} mode long wavelength cut-off

Seongwoo Yoo *, Yongmin Jung, Junki Kim, Jhang W. Lee, Kyunghwan Oh

Department of Information and Communications, Gwangju Institute of Science and Technology (GIST), 1 Oryong-dong, Buk-gu, Gwangju 500-712, South Korea

Received 13 September 2004; revised 4 January 2005

Available online 16 March 2005

Abstract

We propose a novel passive band-pass filtering scheme to obtain a net gain in a band-competing system using a W-type fiber waveguide, slicing a shorter wavelength gain band out of a given stimulated emission cross-section. By controlling the location of the LP_{01} mode cut-off, fiber design parameters are presented for obtaining a U-band gain from Tm ions and S-band from Er ions. The tolerance of the LP_{01} mode cut-off wavelength and the accompanying bending loss are theoretically analyzed in terms of waveguide parameters.
© 2005 Elsevier Inc. All rights reserved.

Keywords: Fiber amplifiers; W-type fiber; S-band amplifier; U-band amplifier

1. Introduction

The increasing demand for wider communication bandwidth has brought in extensive expansion of conventional communication bands into neighboring windows such as S-band (1450–1530 nm) and U-band (1625–1675 nm), and amplifiers for the corresponding bands

* Corresponding author. Present address: Optoelectronics Research Centre, University of Southampton, Southampton, UK. Fax: +44 23 8059 3149.
E-mail address: sey@orc.soton.ac.uk (S. Yoo).

1068-5200/$ – see front matter © 2005 Elsevier Inc. All rights reserved.
doi:10.1016/j.yofte.2005.01.002

are essential for optical networks. The optical fiber amplifiers for S-band were initially developed by gain shifted Tm-doped fluoride fibers using the up-conversion pumping schemes [1]. Recently S-band Er-doped fiber amplifiers (EDFAs) have been reported by suppressing the emission in C-band at longer wavelengths [2,3]. Silica glass host and commercially available components make the S-band EDFA highly competitive yet special waveguide designs or filtering methods are required since the emission cross section of C-band is several times greater than S-band in Er ions. Tm ions show the peak emission cross section near 1.8 μm in a direct three level transition in silica glass [4], and a weak optical gain around 1600–1700 nm covering U-band have been reported in silica based glass fibers [5]. However the competing emission was not effectively suppressed in the report and a higher gain could be expected after filtering out the 1.8 μm band with a special fiber design. Consequently, it is essential to implement versatile methods for suppressing longer wavelengths above S- or U-band in order to achieve optical fiber gain blocks in the bands of interest.

In contrast to conventional step index single mode fibers, W-type fibers have the fundamental LP_{01} mode cut-off at a long wavelength to provide a short wavelength pass filter characteristic as well as negative chromatic dispersion [6–11]. In particular, parametric analysis on waveguide structure and bending loss studies have been established in the silica glass window around 1550 nm for the application of low loss, passive transmission fibers. We will extend the application of W-type fibers to active devices such as fiber amplifiers, where the unique feature of W-fiber, LP_{01} cut-off, is applied in a rare earth doped fiber in order to effectively filter out the competing longer wavelength emission band and achieve a net gain in a shorter wavelength band. In this paper, we present detailed theoretical analyses on W-type fiber designs to obtain S-band out of Er and U-band out of Tm emission cross sections adopting unique short pass characteristics of W-type fibers. Parametric studies on the impact of fiber structural deviation over the location of the LP_{01} mode cut-off wavelength and bending loss of a W-type fiber are theoretically analyzed, for the first time to the best knowledge of the authors. The sensitivity of the cut-off wavelength and bending performances over the W-type fiber parameter variations will provide practical information for design and fabrication of active fibers.

2. Waveguide design for U- and S-band amplifiers

The structure of W-type fiber is illustrated in the inset diagram at the upper left of Fig. 1. It is composed of three layered structure, high refractive index core, depressed inner cladding, and silica cladding. The depressed index cladding is usually achieved by doping fluorine or boron in silica, while the core index is raised by germanium or aluminum. The refractive indices of core, depressed cladding, and outer cladding are denoted as n^+, n^-, and n_0, respectively. The refractive index differences are expressed as $\Delta n^+ = (n^+ - n_0)$ and $\Delta n^- = -(n^- - n_0)$. The core radius is a and the depressed cladding radius is b. These are the key waveguide parameters of a W-type fiber and they will determine guiding properties of the W-fiber.

One of unique properties of W-type fibers is existence of the fundamental LP_{01} mode cut-off [6,8]. As the wavelength increases, the effective index of the fundamental LP_{01}

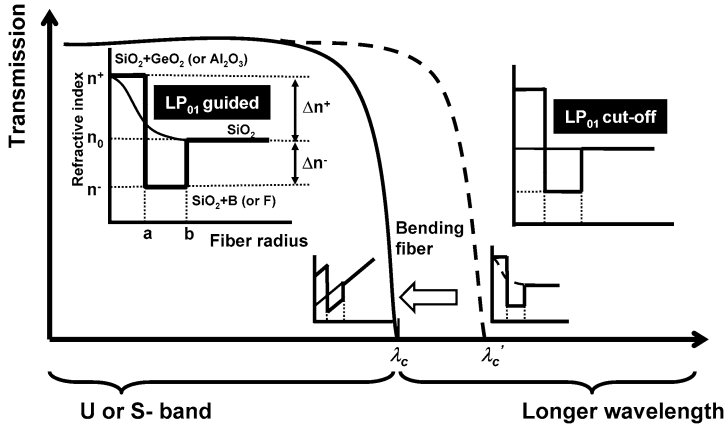

Fig. 1. Structure of W-type fiber and schematics of slicing a desired band by W-type fiber along with fiber bending. The waveguide parameters of W-type fiber are shown in the inset figure on the left hand side. Here n^+, n^-, n_0, a, and b are refractive index of core, depressed cladding, outer cladding, core radius, and depressed cladding radius, respectively. The refractive index differences are expressed as $\Delta n^+ = (n^+ - n_0)$ and $\Delta n^- = -(n^- - n_0)$. By the LP_{01} mode cut-off at λ_c, the signal at $\lambda > \lambda_c$ will be suppressed while the signal at $\lambda < \lambda_c$ will be guided. In addition, the location of λ_c' can be effectively shifted to λ_c by bending the fiber.

mode decreases. At the cut-off wavelength, λ_c, it gets to the value of cladding index then leaks out as a radiation mode as shown in the inset diagram at the upper right of Fig. 1. Therefore, the light whose wavelength is longer than the cut-off can be filtered out passively in a W-type fiber while the shorter wavelength signal experiences negligible loss. This short wavelength-pass filter characteristics will allow us to slice out an appropriate shorter wavelength gain band out of a given emission cross-section of an active ion. However, it is naturally expected that there would be structural deviation of W-type fiber from the initial designs during the fabrication process to result in a deviation of the cut-off wavelength to λ_c', as schematically shown in the horizontal axis of Fig. 1. In order to remedy this deviation, we propose to further bend the fiber in a certain radius of curvature. The macro-bending losses of LP_{01} mode in W-type fibers are significant compared to conventional single step index profile fibers such that circumventing the high losses of W-type fibers had been challenging when considering deploying the fibers [6,12]. The high leakage loss in W-type fibers induced by macro-bending, however, can be taken advantage for our purpose. The bend will affect the effective index structure as shown in the bottom of Fig. 1 and will induce the loss at λ_c' and effectively shift the cut-off from λ_c' to λ_c. Primary mechanisms for effective spectrum slicing in a W-type fiber, therefore, would be locating the LP_{01} mode cut-off by waveguide design and controlling the bend induced loss.

The emission cross-sections of Tm ions [13] in fluoride fibers and Er ions [14] in silica fibers are shown in Fig. 2 along with schematic diagrams for the proposed mechanism to obtain U- and S-band in W-type fibers. By allocating the LP_{01} mode cut-off at an appropriate spectral position, we can filter the competing parts of the emission cross section at the longer wavelength and slice out the desired portion in the shorter wavelength range, U-band (1620–1670 nm) out of Tm ions and S-band (1460–1530 nm) out of Er ions utilizing the short wavelength pass characteristics of W-type fibers.

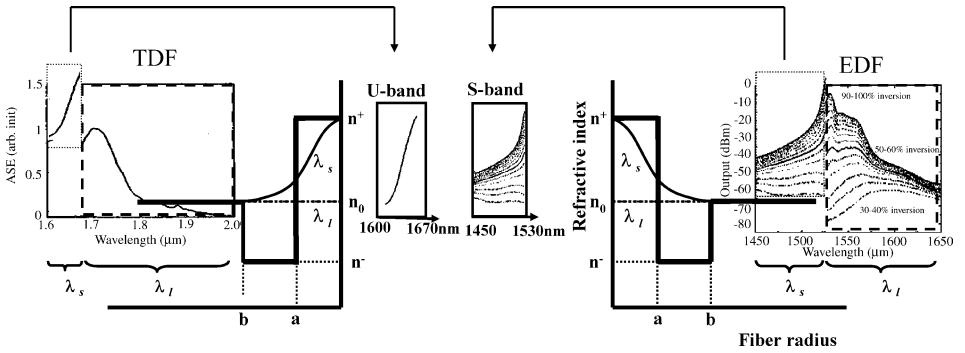

Fig. 2. Schematics for slicing U- and S-band out of the emission cross-sections of Tm-doped fiber (TDF) and Er-doped fiber (EDF), respectively. The emission cross sections are from Refs. [9,10]. Here we presented the W-type fibers where the LP_{01} mode cut-offs are located at the upper bound of U-band, 1670 nm, and that of S-band, 1530 nm. In this condition the signal at a shorter wavelength, λ_s, than λ_c will be guided while the longer wavelength signal λ_s will be cut-off to result in slicing out U- and S-band out of TDF and EDF, respectively.

In this paper the LP_{01} mode cut-off wavelength is calculated in the following procedure. Firstly, the effective index of the LP_{01} mode is obtained at a wavelength by solving vectorial Maxwell's equations for the three-layered structure of W-type fiber along with boundary conditions at the interfaces. The electric field in W-type fiber is given in scalar form as below [8], and the coefficients, A_i, and subsequently the effective index of the mode can be computed by solving Maxwell's equations

$$E(r) = \begin{cases} A_0 J_0(ur/a) & \text{for } r < a, \\ A_1 I_0(w^- r/b) + A_2 K_0(w^- r/b) & \text{for } a < r < b, \\ A_3 K_0(wr/b) & \text{for } r > b, \end{cases} \tag{1}$$

where J_0, I_0, and K_0 are Bessel functions of the first kind, modified Bessel function of the first kind, and the second kind, respectively. The normalized propagation constants, u, w^-, and w are defined as $u = a\{(k_0 n^+)^2 - \beta^2\}^{1/2}$, $w^- = b\{\beta^2 - (k_0 n^-)^2\}^{1/2}$, and $w = b\{\beta^2 - (k_0 n_0)^2\}^{1/2}$, respectively. Here we assumed the core index is raised by germanium and the inner cladding index is depressed by fluorine. The material dispersion of the doped layers was calculated using three term Sellmeir equations for binary germanosilicate glass [15] and F-doped silica [16].

Then the wavelength is scanned until the effective index matches the refractive index of the silica cladding, at which the LP_{01} mode cut-off, λ_c, is evaluated. The routine is repeated for variation of fiber structure parameters to find its impact on the location of λ_c. When we varied one parameter in the analysis, all the rest of waveguide parameters were kept unchanged.

Macro bending loss also affects the output spectrum of a W-type fiber and is described as below in LP_{01} mode [17,18].

$$\alpha = \left(\frac{\pi v^8}{16 a R_b w^3}\right)^{1/2} \exp\left(-\frac{4}{3}\frac{R_b}{a}\frac{w^3\Delta}{v^2}\right)\left[\int_0^\infty \{1-f\}\frac{1}{a^2}F_0 r\,dr\right]^2 \Big/ \int_0^\infty F_0^2 \frac{1}{a^2} r\,dr \tag{2}$$

with refractive index profile function, f,

$$f = \begin{cases} 0, & 0 < r < a, \\ \frac{n^+ - n^-}{n^+ - n_0}, & a < r < b, \\ 1, & r > b \end{cases} \tag{3}$$

and with refractive index parameter, Δ, is given by

$$\Delta = \frac{1}{2}\left(1 - \frac{n_0^2}{n^{+2}}\right), \tag{4}$$

where R_b is bending radius, and F_0 is the electric field magnitude, the solution of Eq. (1). It is expected that the macro-bending losses depend on fiber parameters from Eqs. (3) and (4), which would distinguish the induced bending losses from the one layer step index profile fiber.

Note that the bending loss does depend on wavelength as in Eq. (2) and it can corroborate our proposed spectrum slicing scheme in W-type fiber by inducing higher loss at the longer wavelength. Therefore, firstly the LP_{01} mode cut-off wavelength is controlled by main parameters mentioned previously, and then the parametrically determined fundamental cut-off wavelength is further tuned by imposing macro-bending loss therein.

In order to analyze the effects of waveguide parameters and bending, we have designed W-type fibers by solving Eq. (1) to have the LP_{01} cut-off wavelengths, λ_c, at an appropriate spectral position for U- and S-band applications. Note that we located λ_c at the upper boundary of each band of interest such that W-type fiber for U-band, 1620–1670 nm, had the cut-off at 1670 nm, while that for S-band, 1460–1530 nm, had λ_c at 1530 nm in order to suppress the longer wavelength emission bands. The parameters given in Table 1 were determined by following procedure. Firstly, we set Δn^- as 0.005, which can be achieved by F doping in SiO_2 glass layer in conventional fiber manufacturing process. Then, the core radius, a, was decided as 2 μm so as to match the conventional high power amplifier applications [19]. The cut-off wavelength is, then, determined by controlling b and/or n^+. In W-type fibers, the ratio of refractive index contrast between depressed inner cladding and core, $\Delta n^-/\Delta n^+$, and the ratio of depressed cladding radius to core radius, b/a, are known to characterize the performance [6,8,10]. Once the numerical aperture of the W-fiber is kept as 0.17 as in high power amplifier applications [19], the $\Delta n^-/\Delta n^+$ is consequently assigned to be 0.05. We set $b/a = 3$ in order to provide flexible control of cut-off wavelength [8]. In these conditions, the n^+s are calculated with Eq. (1) to allocate the fundamental mode cut-off wavelengths at 1670 and 1530 nm for U- and S-band, respectively. The W-fiber with $\Delta n^-/\Delta n^+ \sim 0.05$ along with $b/a = 3$ has been known

Table 1
Parameters of calculated W-type fibers for U- and S-band amplifiers

Application band	a (μm)	b (μm)	r_f (μm)	n^+	n^-	n_0	λ_c in LP_{01} mode (nm)
U-band	2	6	62.5	1.4683	1.4520	1.4570	1670
S-band	2	6	62.5	1.4672	1.4520	1.4570	1530

a: Core radius, b: depressed cladding radius from the center, r_f: fiber radius, n^+: refractive index core, n^-: refractive index of depressed cladding, n_0: refractive index of outer cladding, λ_c: cut-off wavelength evaluated from the parameters shown in this table.

to support relatively stable performance against the fundamental mode cut-off wavelength variation [6]. The given parameters in Table 1 were chosen so as to satisfy the requirement for stable guiding performance as well as high power amplifier applications.

For the initial waveguide parameters in Table 1, we investigated the effects of bending in W-fibers by estimating the bend induced loss at the upper and lower boundary of the bands of interests, 1620 and 1670 nm for U-band fiber and at 1460 and 1530 nm for S-band. The change of bending loss was theoretically predicted for variations in fiber parameters.

3. The LP_{01} mode cut-off wavelength versus variations in fiber parameters

3.1. Impact of core parameters on cut-off wavelength

For the given fiber structures of U- and S-band fibers in Table 1, firstly the core radius, a, and core refractive index, n^+, is varied by Δa and Δn^+, respectively and then the impacts of the relative variation $\Delta a/a$ and $\Delta n^+/n^+$ over the LP_{01} mode cut-off wavelength, λ_c, are analyzed and the results are shown in Fig. 3. Considering the state of art fabrication, the curves of λ_c are plotted in the region of $-5 < \Delta a/a < 5\%$, corresponding to ± 0.1 μm variation in a in Fig. 3a and in the region of $-0.034 < \Delta n^+/n^+ < 0.034\%$, ± 0.0005 variation in n^+, in Fig. 3b. In both U- and S-band fibers, λ_c significantly shifts to

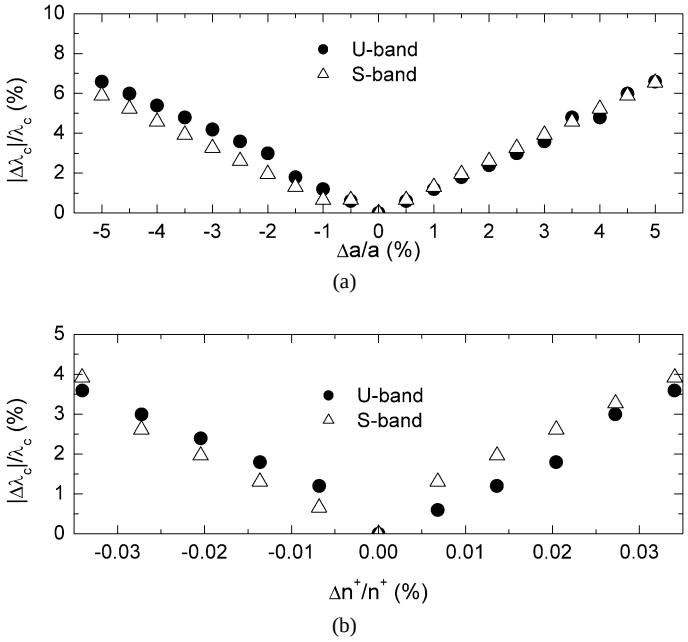

Fig. 3. Dependence of the LP_{01} mode cutoff wavelengths, λ_c, on the variation of (a) core radius, $\Delta a/a$, and (b) core refractive index, $\Delta n^+/n^+$, in U- and S-band. Here for the negative $\Delta a/a$ and $\Delta n^+/n^+$, λ_c decreases and its relative magnitude is plotted. The λ_c is 1670 and 1530 nm in U- and S-band, respectively, when $\Delta a/a$ and $\Delta n^+/n^+ = 0$. The initial fiber parameters are given in Table 1.

a longer wavelength with increasing core parameters and shifts to a shorter wavelength for decreasing core parameters in a linear manner.

For 5% increment of $\Delta a/a$, the λ_c increases as high as 1780 nm from 1670 nm in U-band. The λ_c decreases to 1560 nm for -5% of $\Delta a/a$. The curves were linearly fitted to find the slope of the λ_c variation. In U-band, the slope, $(|\Delta\lambda_c|/\lambda_c)/(\Delta a/a)$, in the case of $\Delta a/a < 0$ is around -1.35 and the curve in the case of $\Delta a/a > 0$ shows a similar slope about 1.32.

The magnitude of the shift of λ_c is reduced in the case of S-band. The $\pm 5\%$ variation in $\Delta a/a$ gives rise to change of λ_c in the range 1440–1630 nm. The slopes of the curves in S-band are -1.2 when $\Delta a/a < 0$ and 1.30 when $\Delta a/a > 0$.

For the variation of n^+, in U-band, the λ_c increases as high as 1730 nm from 1670 nm for 0.034% increment of $\Delta n^+/n^+$ and it decreases to 1610 nm for -0.034% of $\Delta n^+/n^+$. The curves were also linearly fitted to find the slope of the λ_c variation. The slopes, $(|\Delta\lambda_c|/\lambda_c)/(\Delta n^+/n^+)$, in the region of $\Delta n^+/n^+ < 0$ are around -100 and -110 in U- and S-band, respectively, and the curves in the case of $\Delta n^+/n^+ > 0$ have very similar slopes about 108 and 110 in U- and S-band, respectively.

As shown in Fig. 3, λ_c is very sensitive to the variation of a as well as n^+. Using the linear fits, the variations in λ_c corresponding to increase in the core radius by 0.1 μm are estimated as 120 and 106 nm for U- and S-band, respectively. It was also found that the inaccuracy by 0.0005 in n^+ will induce λ_c shift around 60 nm in both of U- and S-band. Even in the state of art fabrication, 0.1 μm inaccuracy of core radius could be commonly encountered but the corresponding cut-off wavelength shift around 100 nm would cause practical problem to precisely locate λ_c at a desired spectral position.

In order to circumvent this fabrication limitation, we propose that a W-type fiber structure and macro-bending be simultaneously employed. In this proposed technique, a W-type fiber with a larger core and/or higher n^+ within an allowed range is fabricated and the signal at a longer wavelength than the target λ_c is furthermore suppressed by bending loss, see Fig. 1. Note that bending loss grows exponentially with increasing wavelength for a small bending radius [20] and W-fiber under the macrobending will further suppress the long wavelength signals while maintaining high transparency in the desired shorter wavelength bands. Note that the given parameters were carefully determined to stabilize the performance against LP_{01} cut-off wavelength. Therefore, the resulted λ_c shift can be easily expected in practice.

3.2. Impact of depressed inner cladding parameters on cut-off wavelength

Shifts in λ_c for the relative inner cladding radius variation, $\Delta b/b$, and refractive index, $\Delta n^-/n^-$, are calculated for U- and S-band and the results are shown in Fig. 4. Initially, the variations of b and n^- are ranged in $5.9 < b < 6.1$ μm corresponding to $-1.7 < \Delta b/b < 1.7\%$, and $1.4515 < n^- < 1.4525$, corresponding to $-0.034 < \Delta n^-/n^- < 0.034\%$, respectively, considering fiber fabrication errors. In Fig. 4a the depressed cladding radius, b, expands up to 12 μm (100%) from 5.4 μm (-10%) to investigate the behavior of λ_c for $\Delta b/b$.

Compared with the behavior of λ_c with respect to the variation in the core radius, Fig. 4a shows very different nature. The cut-off wavelength, λ_c, monotonically decreases step-wise

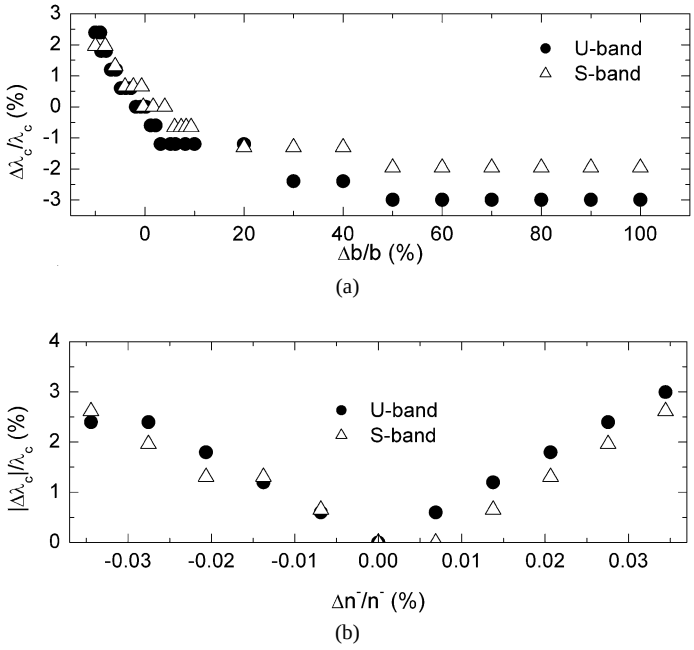

Fig. 4. Dependence of the LP_{01} mode cutoff wavelengths, λ_c, on the variation of (a) depressed cladding radius, $\Delta b/b$, and (b) refractive index, $\Delta n^-/n^-$, in U- and S-band. Here for the negative $\Delta n^-/n^-$, λ_c decreases and its relative magnitude is plotted. The λ_c is 1670 and 1530 nm in U- and S-band, respectively, when $\Delta b/b$ and $\Delta n^-/n^- = 0$. The initial fiber parameters are given in Table 1.

for increasing $\Delta b/b$ until $\Delta b/b$ reaches 50%. When the inner cladding is expanded more than 50% of the initial value, $\Delta b/b > 50\%$, $\lambda_c s$ do not change any more and they stay at 1620 and 1500 nm for U- and S-band, respectively. It is noteworthy that the amount of λ_c shift is much less significant compared to that in the case of core radius dependence. In both of U- and S-band, λ_c shift is considerably reduced to be about 5 nm for the change in b by 0.1 μm in the range of $-1.7\% < \Delta b/b < 1.7\%$, which is only a fraction compared to the λ_c shift by $\Delta a/a$.

The shifts in λ_c for the relative variation of the refractive index of inner cladding, $\Delta n^-/n^-$, are also shown in Fig. 4b. The λ_c shifts to longer wavelength with increasing $\Delta n^-/n^-$ and shows steeper increase for $\Delta n^-/n^- > 0$. The slopes of the curves with linear fitting produce 40 and 50 nm shift in λ_c for 0.0005 deviation of n^- in the region of $-0.034 < \Delta n^-/n^- < 0\%$ and $0 < \Delta n^-/n^- < 0.034\%$, respectively, in U-band. In S-band, the linearly fitted slopes give rise to λ_c shift in 30 and 50 nm for 0.0005 variation in n^- in the region of $-0.034 < \Delta n^-/n^- < 0\%$ and $0 < \Delta n^-/n^- < 0.034\%$, respectively.

The λ_c shift depending on the parameters of depressed inner cladding is significantly reduced in particular on the depressed cladding radius compared to the case of core parameters. Nonetheless, the variation of the refractive index of depressed cladding is found to cause considerable shift in λ_c. Therefore, the bending loss should be considered to suppress any expected longer wavelength guidance in W-fibers induced by the variation of n^-.

4. Macrobending for the longer wavelength signal suppression and its dependence on the variation of parameters

The macro bending in the proposed W-fibers is plotted against the core diameter variation, $\Delta a/a$, for the various bending radii, R, in Fig. 5. The bending loss grows as $\Delta a/a$ and R decrease. Moreover, the bending loss at the longer wavelength, 1670 nm for U-band and 1530 nm for S-band, is greater than at the shorter wavelength, 1620 nm for U-band and 1460 nm for S-band, by orders of magnitude. Due to this differential bending loss we can keep the bending loss in the bands of interests negligible while effectively inducing a large bending loss to suppress the wavelengths beyond the band.

In Fig. 5a, when $\Delta a/a$ is 5%, the bending losses at 1620 and 1670 nm with $R = 18$ mm are 10^{-3} and 60 dB/m, respectively. Assuming that the fiber length of 10 m is wound on a post of $R = 18$ mm, signal beyond 1670 nm will be effectively suppressed by bending loss over 600 dB while keeping a high transparency of 0.1 dB at 1620 nm. Now if $\Delta a/a$ is smaller than 1.5%, the bending radius of 18 mm is too tight to result in high loss at both 1620 and 1670 nm and a larger bending radius is necessary. For $\Delta a/a = 1.5\%$, $R = 23$ mm is preferred to support U-band transparency. Figure 5b depicts the bending loss of W-type S-band fiber with the bending radii of 15 and 20 mm. Assuming S-band fiber of 10 m long and $\Delta a/a$ of 5%, the bending radius of 15 mm will induce a loss below 0.1 dB at 1460 nm

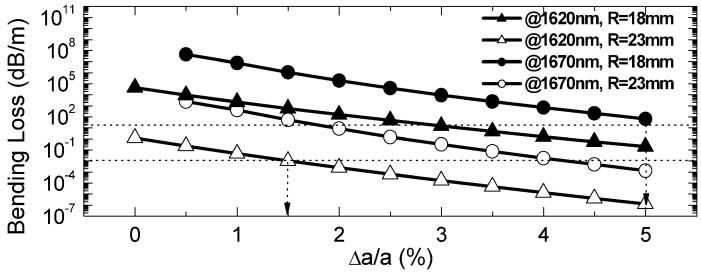

(a)

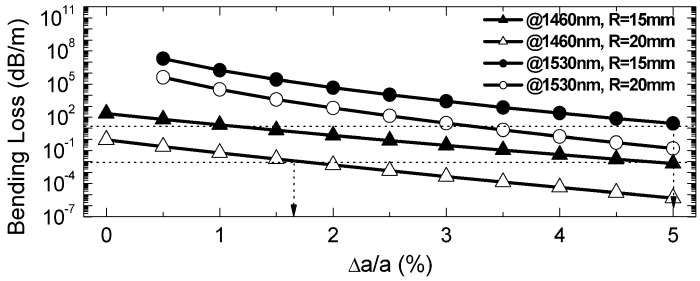

(b)

Fig. 5. Bending loss of W-type (a) U-band fiber at the boundary of the band, 1620 and 1670 nm and (b) S-band fiber at the boundary of the band, 1460 and 1530 nm. Under the lower horizontal line at 10^{-2} dB/m, the transparency in each band is maintained while longer wavelength than each band is suppressed above the upper horizontal line at 20 dB/m with 10 m long W-type fibers.

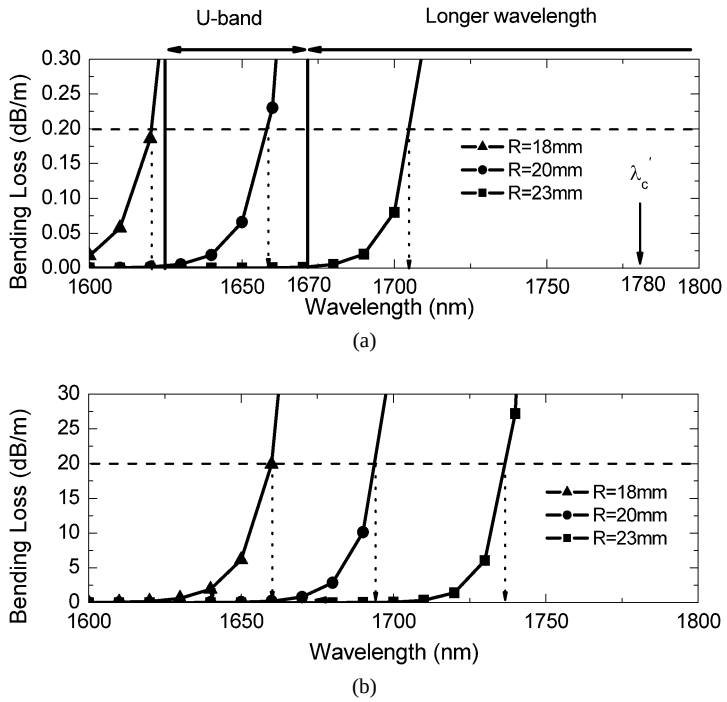

Fig. 6. Bending loss vs wavelength in U-band W-fiber. λ_c' is deviated cut-off wavelength induced by 5% variation in $\Delta a/a$. The horizontal lines in (a) and (b) indicate the effective cut-off condition and the complete suppression above U-band with 10 m fiber length, respectively.

while more than 200 dB loss at wavelength over 1530 nm. When the variation $\Delta a/a$ is smaller than 1.7%, the S-band failed to be transparent for $R = 15$ mm and a bending radius larger than 20 mm is required. Note that the fiber length of 10 m is arbitrary but it is representing actual fiber length in rare earth-doped fiber amplifiers. Two horizontal dotted lines are added on Fig. 5, which correspond to the bending losses of 10^{-2} and 20 dB/m. These will serve as a guide line for 10^{-1} dB loss for the band of interest and 200 dB loss for signal beyond the band [2].

In Fig. 5, we have confirmed that bending the W-fibers will provide ability to control the cut-off wavelength. In order to further analyze the shift of λ_c in spectral domain, we calculated the bending loss as a function of wavelength for various bending radii as in Figs. 6 and 7. Here we will examine specific cases such that we have $\Delta a/a = 5\%$, which will shift the cut-off wavelength to λ_c'. By applying bending to this fiber of 10 m long, we will induce wavelength dependent bending loss to result in effective λ_c shift toward the shorter wavelength as illustrated in Fig. 1. As the cut-off wavelength is conventionally determined at the point where the maximum transmitted power drops by 2 dB [21], we drew 0.2 dB/m horizontal line in Figs. 6a and 7a, to determine the effective cut-offs for different bending radii. In Figs. 6b and 7b with a larger vertical scale, we also drew 20 dB/m horizontal line, to estimate the long wavelength from which fiber bending will induce loss more than 200 dB.

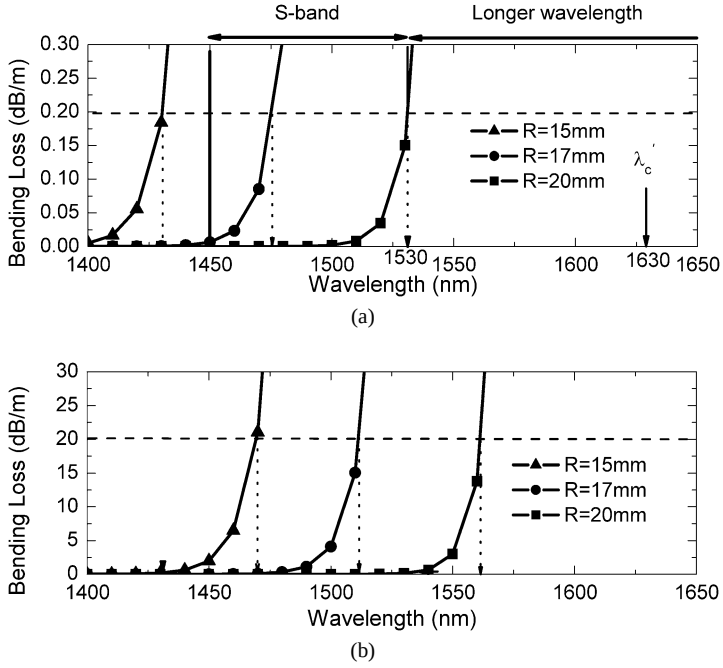

Fig. 7. Bending loss vs wavelength in S-band. λ_c' is the deviated cut-off wavelength induced by 5% variation in $\Delta a/a$. The horizontal lines in (a) and (b) indicate the effective cut-off condition and the complete suppression above S-band with 10 m fiber length, respectively.

For U-band, $\Delta a/a = 5\%$ result in $\lambda_c' = 1780$ nm. Figure 6a illustrates that the effective cut-off wavelength does depend on bending radii. The effective cut-off wavelength moves to 1705, 1660, and 1620 nm for $R = 23, 22$, and 18 mm, respectively. However, the cut-off shift alone is not enough to suppress the competing emission at the longer wavelength and we need to confirm more than 200 dB loss beyond the band of interests as recommended in Ref. [2]. In Fig. 6b, losses over 200 dB are achieved in 10 m long W-fibers above 1735, 1695, and 1660 nm for $R = 18, 20$, and 18 mm, respectively. These results clearly show that the bending loss provides an effective post-fiber fabrication technique to control the LP_{01} mode cut-off wavelength of W-fiber as well as to suppress the longer wavelength above the band of interests, compensating the deviation of λ_c by $\Delta a/a$ of 5%.

For S-band, $\Delta a/a = 5\%$ result in $\lambda_c' = 1630$ nm. In Fig. 7a, the effective cut-off wavelength moves to 1530, and down to 1430 nm for $R = 20$ and 15 mm, respectively. Figure 7b shows the condition of further suppression of the wavelengths above S-band with different bending radius. Over 200 dB losses are induced in the longer wavelengths above S-band by bending W-fibers with $17 < R < 20$ mm. Similar to Fig. 6, we found that fiber bending will provide an effective method to overcome waveguide parameter variations and subsequent changes in cut-off wavelength and suppress the competing emission in the longer wavelengths.

Figure 8 shows the dependences of bending losses on $\Delta n^+/n^+$. Note that the curves were not plotted in the region where the LP_{01} mode cut-off condition is met by the variation

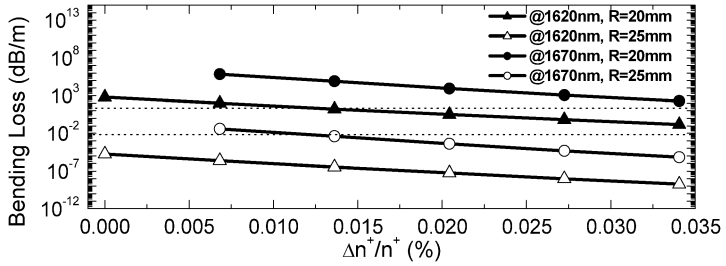

(a)

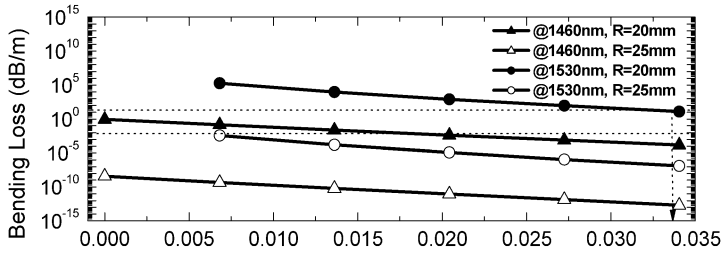

(b)

Fig. 8. Bending losses of W-type (a) U-band fiber and (b) S-band as a function of the relative core refractive index variation, $\Delta n^+/n^+$. Under the lower dotted horizontal line at 10^{-2} dB/m, the transparency in each band is maintained while the longer wavelength signal is suppressed above the upper dotted horizontal line at 20 dB/m for 10 m long W-type fibers.

Δn^+, because it is not meaningful to calculate the bending loss for leaky modes beyond the cut-off condition. In Fig. 8, it is shown that R between 20 and 25 mm significantly suppresses the longer wavelength as indicated by the upper dotted horizontal line, maintaining high transparency in U- and S-band, bounded by the lower horizontal line, for 10 m long W-type fibers. Therefore, the cut-off shift induced by the fabrication inaccuracy up to 0.0005 in refractive index of the core, $\Delta n^+/n^+ = 0.034\%$, can be recovered by winding 10 m long fibers on a post of bending radius $20 < R < 25$ mm for both U- and S-band W-fibers.

Figure 9 shows the dependences of bending losses on $\Delta n^-/n^-$. Similarly to Fig. 8, the curves were not plotted in the region where the LP_{01} mode cut-off condition is met by the variation Δn^-. It is found the variation of $\Delta n^-/n^-$ induces less significant changes in the bending loss compared with the variation induced by $\Delta n^+/n^+$. The bending losses at the shorter boundaries, 1620 nm for U-band and 1460 nm for S-band were almost kept unchanged regardless of the variation of $\Delta n^-/n^-$. At the longer boundaries, 1670 nm for U- band and 1530 nm for S-band, the bend-induced losses in a relatively wide range were obtained for different bending radii. It is found that the fabrication error in n^- by 0.0005 can be compensated by bending the fiber with $20 < R < 25$ mm.

In Figs. 5, 8, and 9, it was found that the dependences of bending losses on core parameters are more significant than on depressed cladding parameters. Moreover, we found that the normal deviations in n^+ and n^- occurred in conventional fabrication process, can

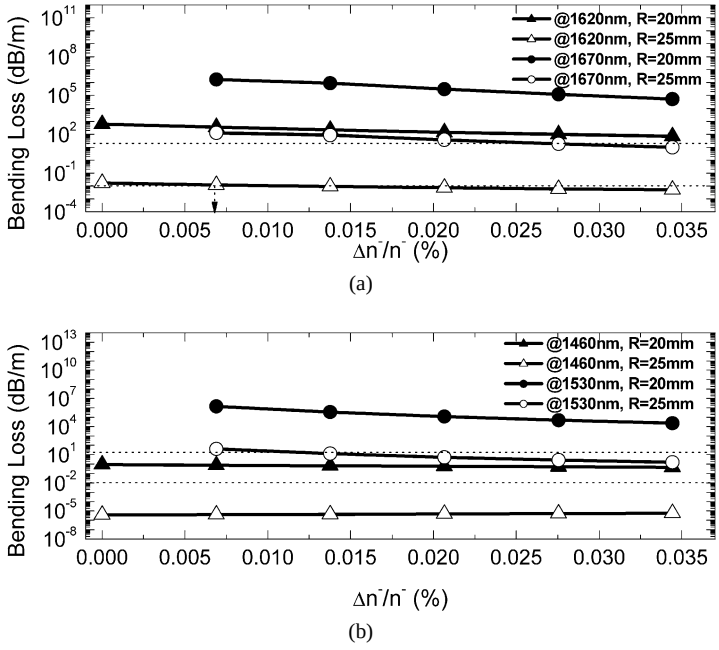

Fig. 9. Bending losses of W-type (a) U-band fiber and (b) S-band as a function of the relative depressed cladding refractive index variation, $\Delta n^{-}/n^{-}$. Under the lower dotted horizontal line at 10^{-2} dB/m, the transparency in each band is maintained while the longer wavelength signal is suppressed above the dotted upper horizontal line at 20 dB/m for 10 m long W-type fibers.

be effectively compensated bending the fiber in a radius range of $20 < R < 25$ mm. On the while, the deviation in a requires a tighter bending radius such as $18 < R < 23$ mm in U-band and $15 < R < 20$ mm in S-band.

5. Conclusion

The fundamental mode cut-off behavior in W-type fibers was theoretically investigated in terms of parameters along with bending loss for the purpose of modifying emission cross section and subsequently slicing U-band out of thulium and S-band from erbium. Shift in the LP_{01} mode cut-off wavelength as well as macro-bending loss was found to depend more heavily on the core parameters than the inner-cladding parameters. Bending the W-fiber in an appropriate range of radius was found to provide an effective measure to compensate the cut-off wavelength shift induced by fabrication inaccuracy and furthermore enhance the longer wavelength signal suppression inducing wavelength dependent bending loss. In particular, the fabrication error by 0.1 μm in the core radius and 0.0005 in the refractive index of core, usually met in conventional fiber manufacturing process, were found to be effectively compensated by bending the fiber with the radius near 20 mm. The results strongly suggest that a gain band in the shorter wavelength can be sliced out from the given emission cross-section of a rare earth ion in fibers using W-type design along with

an appropriately deigned bending loss mechanism. This proposed technique can be applied in novel design of active rare earth doped fiber devices.

References

[1] T. Komukai, T. Yamamoto, T. Sugawa, Y. Miyajima, Upconversion pumped Tm-doped fluoride fiber amplifier and laser operating at 1.47 μm, J. Quant. Electron. 31 (1995) 1880–1889.
[2] M. Arbore, Y. Zhou, H. Thiele, J. Bromage, L. Nelson, S-band Er-doped fiber amplifiers for WDM transmission between 1488 and 1508 nm, in: Proc. OFC 2003, Washington, DC, 2003, pp. 374–376, paper WK2.
[3] M. Arbore, Y. Zhou, G. Keaton, T. Kane, >30 dB gain at 1530 nm in S-band Er-doped silica fiber with distributed ASE suppression, in: Proc. of SPIE, Optical Devices for Fiber Communication, vol. IV, 2003, pp. 47–52, paper 4989.
[4] S.D. Jackson, T.A. King, Theoretical modeling of Tm-doped silica fiber lasers, J. Lightwave Technol. 17 (1999) 948–956.
[5] I. Sankawa, H. Izumita, S.-I. Furukawa, K. Ishihara, An optical fiber amplifier for W-band wavelength range around 1.65 μm, Photon. Technol. Lett. 2 (1990) 422–424.
[6] L.G. Cohen, D. Marcuse, W.L. Mammel, Radiating leaky-mode losses in single-mode lightguides with depressed-index claddings, Trans. Microwave Theory Tech. MTT-30 (1982) 1455–1460.
[7] T. Miya, K. Okamoto, Y. Ohmori, Y. Sasaki, Fabrication of low dispersion single-mode fibers over a wide spectral range, J. Quant. Electron. QE-17 (1981) 858–861.
[8] M. Monerie, Propagation in doubly clad single-mode fibers, J. Quant. Electron. QE-18 (1982) 535–542.
[9] P. Francois, Tolerance requirements for dispersion free single-mode fiber design: Influence of geometrical parameters, dopant diffusion, and axial dip, Trans. Microwave Theory Tech. MTT-30 (1982) 1478–1487.
[10] H.J. Hagemann, H. Lade, J. Wamier, D. Wiechert, The performance of depressed-cladding single-mode fibers with different b/a ratio, J. Lightwave Technol. 9 (1991) 689–694.
[11] J. Auge, C. Brehm, L. Jeunhomme, C.L. Sergent, Parametric study of depressed inner cladding single-mode fibers, J. Lightwave Technol. LT-3 (1985) 767–772.
[12] D. Marcuse, Influence of curvature on the losses of doubly clad fibers, Appl. Opt. 21 (23) (1982) 4208–4213.
[13] T. Sakamoto, M. Shimizu, M. Yamada, T. Kanamori, Y. Ohishi, Y. Terunuma, S. Sudo, 35-dB gain Tm-doped ZBLYAN fiber amplifier operating at 1.65 μm, Photon. Technol. Lett. 8 (1996) 349–351.
[14] Y. Im, Athermalization of EDFA by serial concatenations of antimony-doped silica fiber in conventional band, MS dissertation, 2003.
[15] J.W. Fleming, Dispersion in GeO_2–SiO_2 glasses, Appl. Opt. 23 (1984) 4486–4493.
[16] J.W. Fleming, D.L. Wood, Refractive index dispersion and related properties in fluorine doped silica, Appl. Opt. 22 (1983) 3102–3104.
[17] A.W. Snyder, J.D. Love, Optical Waveguide Theory, Chapman & Hall, New York, 1983, p. 474.
[18] S.J. Garth, Modes and propagation constants on bent depressed inner cladding optical fibers, J. Lightwave Technol. 7 (1989) 1889–1894.
[19] P.C. Becker, N.A. Olsson, J.R. Simpson, Er-doped Fiber Amplifiers, Academic Press, San Diego, 1999, ch. 8.
[20] D. Marcuse, Bend loss of slab and fiber modes computed with diffraction theory, J. Quant. Electron. 29 (1993) 2957–2961.
[21] F.C. Allard, Fiber Optics Handbook for Engineers and Scientists, McGraw–Hill, New York, 1990, ch. 4.